**1**

# A Hydroinformatic Tool for Sustainable Estuarine Management

António A.L.S. Duarte
*University of Minho*
*Portugal*

## 1. Introduction

Hydrodynamics and pollutant loads dispersion characteristics are determinant factors for an integrated river basin management, where different waters uses and aquatic ecosystems protection must be considered. Strategic Environmental Assessment (SEA) of river basin planning process is crucial to promote a sustainable development. Towards this purpose, the European Water Framework Directive (WFD) establishes a scheduled strategy to reach good ecological status and chemical quality for all European water bodies.

As transitional aquatic environments, where fresh and marine waters meet, estuaries are generally characterized by complex interactions, with strong gradients and discontinuities, between physical, chemical and biological processes. This complexity is often increased by intensive anthropogenic inputs (nutrients and pollutants) from urban, agricultural and industrial effluents, leading to sensitive structural changes (Paerl, 2006) that modify both the trophic state and the health of the whole estuarine ecosystem. As a response to this, there has been an enormous increase in restoration plans for reversing habitat degradation, based on knowledge of the processes which led to the observed ecological changes (Valiela et. al., 1997).

Estuaries are recognised worldwide for providing essential ecological functions (fish nursery, decomposition, nutrient cycling, and shoreline protection) and support multiple human activities (fisheries resources, harbours, and recreational purposes). Each estuary is unique, because of its specific geological structure, morphology, hydrodynamics, land use, and the inflowing freshwater´s characteristics (amount and quality).

Estuarine waters are generally characterized by intense biogeochemical processes that can renew the aquatic compartment, but their flushing capacity is mainly dependent on the hydrodynamic processes. The major driving forces of estuarine circulation are tides, wind, freshwater inflow, and general morphology (bathymetry, intertidal areas extension, roughness). The mixing and dispersion processes are critically dependent upon the salinity intrusion type (concerning it spatial distribution), which defines estuaries ranging from those with a highly stratified salt-wedge and a sharp halocline in the vertical structure to well-mixed systems.

The description of the estuarine transport process can be expressed by the definition of a transport time scale. This time scale is generally shorter than the time scale of the biogeochemical renewal processes and gives an estimate of the water-mass retention within the river basin system. So, the influence of hydrodynamics must not be neglected on

estuarine eutrophication vulnerability assessment, because flushing time is determinant for the transport capacity and the permanence of substances, like pollutants or nutrients, inside an estuary (Duarte, 2005).

Excessive nutrient input, associated with high residence times, leads to eutrophication of estuarine waters and habitat degradation. It is widely recognized as a major worldwide threat, originating sensitive structural changes in estuarine ecosystems due to strong stimulation of opportunistic macroalgae growth, with the consequent occurrence of algal blooms (Pardal et al., 2004).

Much progress has been made in understanding eutrophication processes and in constructing modelling frameworks useful for predicting the effectiveness of nutrient reduction strategies (Thomann & Linker, 1998) and the increase of the estuarine flushing capacity in order to reverse habitat degradation, based on knowledge of the major processes that drive the observed ecological changes (Duarte et. al., 2001).

Residence time (RT) is a concept related with the water constituents (conservatives or not) permanence inside an aquatic system. Therefore, it could be a key-parameter towards the sustainable management of estuarine systems, because its values can represent the time scale of physical transport and processes, and are often used for comparison with time scales of biogeochemical processes, like primary production rate (Dettmann, 2001). In fact, estuaries with nutrients residence time values shorter than the algal cells doubling time will inhibit algae blooms occurrence (Duarte & Vieira, 2009a).

Estuarine water retention (or residence) time (WRT) has a strong spatial and temporal variability, which is accentuated by exchanges between the estuary and the coastal ocean due to chaotic stirring at the mouth (Duarte et. al., 2002). So, the concept of a single WRT value per estuary, while convenient from both ecological and engineering viewpoints, is shown to be an oversimplification (Oliveira & Baptista, 1997). The WRT (so called as transport time scale) has been assessed by many authors to be a fundamental parameter for the understanding of the ecological dynamics that interest estuarine and lagoon environments (Monsen et al., 2002).

The WRT variability within the basin has been related, in many research works, with the variability of some important environmental variables (dissolved nutrient concentrations, mineralization rate of organic matter, primary production rate, and dissolved organic carbon concentration). In literature, the WRT is defined through many different concepts: age, flushing time, residence time, transit time and turn-over time. Nevertheless, the definitions of these concepts are often not uniquely defined and generally confusing.

WRT estimation can be done considering an Eulerian or a Lagrangian approach. In the first option, WRT is identified as the time required for the total mass of a conservative tracer originally within the whole or a segment of the water body to be reduce to a factor "1/e" (Sanford et al., 1992; Luketina, 1998, Wang et al., 2004; Rueda & Moreno-Ostos, 2006; Cucco & Umgiesser, 2006), being a property of a specific location within the water body that is flushed by the hydrodynamic processes. In the second one, it is identified as the water transit time that corresponds to the time it takes for any water particles of the sample to leave the lagoon through its outlet (Dronkers & Zimmerman, 1982; Marinov & Norro, 2006; Bendoricchio, 2006), being a property of the water parcel that is carried within and out of the basin by the hydrodynamic processes.

The two methods give similar results for transport time scales calculation only when applied to simple cases, such as regular basins or artificial channels (Takeoka, 1984). However, sensitive differences arise in applications to basins characterized by complex morphology

and hydrodynamics, mostly induced by the tidal range variability. It should be noted that the Lagrangian technique used for water transport time computation neglects the return flow effect at the estuarine mouth, which does not happen with the Eulerian approach. So, from a hydrological analysis in order to understand the flushing capacity of a tidal embayment, the Eulerian transport time scale seems to be the most representative parameter of all the processes occurring in the basin (Cucco et. al., 2009) and, being less dependent of tide variability, is able to describe the long term flushing dynamics of an estuarine system.

A numerical modelling study applied to Tampa Bay (Florida) was performed comparing the residence times by this two different methods: Eulerian concentration based, and Lagrangian particle tracking. The results obtained with the Lagrangian approach showed a doubling of overall residence time and strong spatial gradients in residence time values (Burwell, 2001).

Since the lower WRT values can increase the estuarine eutrophication processes, an enhanced Eulerian approach was adopted in this research study, conceptualising the residence time (RT) as a characteristic of water constituents, also including the no conservative substances. Thus, RT values were calculated, for each location and instant, as an interval of time that is necessary for that corresponding initial mass to reduce to a pre-defined percentage of that value, using the developed *TemResid* module (Duarte, 2005). In this work, a value of 10% was defined for the residual concentration of the substance, attending to the fact that the effect of the re-entry of the mass in the estuary during tidal flooding is considered (a significant effect for dry-weather river flow rates).

Mathematical models are well known as useful tools for water management practices. They can be applied to solve or understand either simple water quality problems or complex water management problems of estuaries, trans-boundary rivers or multiple-purpose and stratified reservoirs. Accidental spills of pollutants are of general concern and could be harmful to water users along the river basins, becoming crucial to get knowledge of the dispersive behaviour of such pollutants.

In this context, the mathematical modelling of dispersion phenomena can play an important role. Additionally, a craterous selection of mathematical models for application in a specific river basin management plan can mitigate prediction uncertainty. Therefore, intervention measures and times will be established with better reliability and alarm systems could efficiently protect the aquatic ecosystems, the water uses and the public health (Duarte & Boaventura, 2008). The benefits of the synergy between modelling and monitoring are often mentioned by several authors and the linkage of both approaches makes possible to apply cost-benefit measures (Harremoës & Madsen, 1999). Therefore, it is essential to correlate monitoring and modelling information with a continuous feedback, in order to optimize both processes, the monitoring network and the simulation scenarios formulation.

An integrated approach (hydrodynamics and water quality issues) is fundamental to prioritise risk reduction options in order to protect water sources and to get a high quality of the raw material for the water supply systems (Vieira et. al., 1999). Moreover, integrated models allow the optimization of the designed monitoring network (Fig. 1, adopted from Stamou et. al., 2007), based on hydrodynamic and water quality parameters calculation at any section using data from a monitoring programme (necessarily applied to limited number of sampling or measuring stations).

The analysis of water column and benthos field data observed in the Mondego estuary (Portugal), over the last two decades, allowed us to conclude that hydrodynamics was a major factor controlling the occurrence of macroalgae blooms, as determinant of nutrients

availability and uptake conditions (Martins et al., 2001). Thus, the development of hydrodynamic (transport) processes characterization was obviously pertinent and useful.
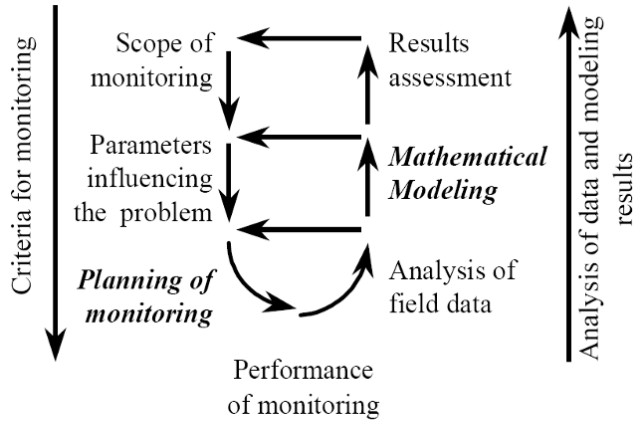


Fig. 1. Interaction between monitoring and modelling for monitoring network optimization

The aims of this chapter are to present the structure of a hydroinformatic tool developed for the Mondego estuary − named *MONDEST model* − linking hydrodynamics, water quality and residence time calculation modules, in order to simulate estuarine hydrodynamic behaviour, salinity and residence times spatial distributions, at different simulated management scenarios. Model calibration and validation was performed using field data obtained from the sampling carried out over the past two decades (Duarte, 2005).The results of the model simulations, considering different river water flow scenarios, illustrate the strong asymmetry of flood and ebb duration time at the inner sections of this estuary, a key-parameter for a correct tidal flow estimation, as the major driving force of the southern arm flushing capacity. The saline wedge propagation into the estuary and the spatial variation of residence time values are also assessed under different management scenarios. The RT values obtained show a strong spatial and temporal variability, as expected in complex aquatic ecosystems with extensive intertidal areas (Duarte & Vieira, 2009b)

The conclusion of this chapter will confirm the crucial influence of hydrodynamics on estuarine water quality status (chemical and ecological) and the usefulness of this hydroinformatic tool as contribution to support better management practices and measures of this complex aquatic ecosystem, like nutrient loads reduction or dislocation and hydrodynamic circulation improvement, in order to contribute for a true sustainable development.

## 2. Methods

### 2.1 Study site

The Mondego river basin is located in the central region of Portugal. The drainage area is about 6670 km² and the annual mean rainfall is between 1000 and 1200 mm. The area covered in this study refers to the whole Mondego estuary (Fig. 2), 32 km in length from its ocean boundary defined approximately 3 km outward from the mouth to Pereira bridge.

Fig. 2. Location and layout of river Mondego estuary

This complex and sensitive ecosystem was under severe environmental stress due to human activities: industries, aquaculture farms and nutrients discharge from agricultural lands of low river Mondego valley.

The Mondego estuary main zone (40°08'N 8°50'W), with only about 10 km long, is divided into two arms (north and south) with very different hydrological characteristics, separated by the Murraceira Island (Fig. 3).



Fig. 3. Aerial views of Mondego estuarine main zone

The north arm is deeper and receives the majority of freshwater input (from Mondego River), while the south arm of this estuary is shallower (2 to 4 m deep, during high tide) and presents an extensive intertidal zone covering almost 75% of its total area during the ebb tide. The irregularity of its morphology and bathymetry is depicted in Fig. 4 (Duarte, 2005).
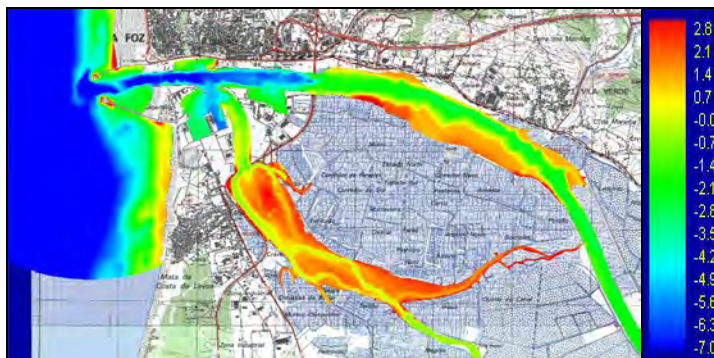


Fig. 4. The Mondego estuary (main zone) bathymetry

For some decades, the river Mondego estuary was under severe ecological stress, mainly caused by eutrophication of its south arm due to the combination of the nutrient surplus with low hydrodynamics and high salinity, because, until the end of 1998, this sub-system was almost silted up in the upstream areas (Fig. 5), drastically reducing the Mondego river water inflow. Hence, the south arm estuary water circulation was mainly driven by tide and wind, originating, in dry-weather conditions, a coastal lagoon-like behaviour. The freshwater inflow was seasonal and only provided by the (small) discharges of the Pranto River, a tributary artificially controlled by the *Alvo* sluices, located 1 km upstream from its mouth.

The most visible effect of this important hydrodynamic constrain was the occurrence of episodic macroalgae blooms and the concomitant severe decrease of the area occupied by *Zostera noltii* beds. So, for the control of this eutrophication process, it became crucial to obtain field data to characterize the real trophic status of this aquatic ecosystem, as well as to better understand the major mechanisms that regulate the abundance of opportunistic macroalgae in order to eradicate its periodic early spring algal blooms.



Fig. 5. Silting up process occurred in the upstream areas of the estuary south arm

Figure 6 shows the size-grain distribution of the sediments in the Mondego estuary main zone (Cunha & Dinis, 2002). A strong correlation was found with the flow channels configuration that occurs during low tide. This information could be very useful for the roughness coefficient definition along the estuarine system, considering or not the variability of the bottom shear stress.
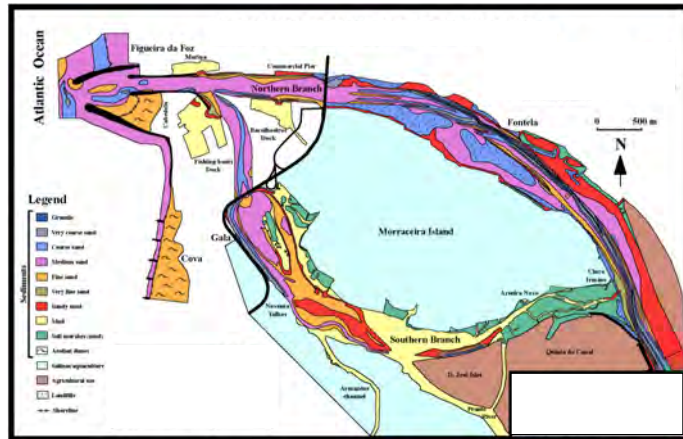
Fig. 6. Mondego estuary grain-size map

The Mondego River monthly inflows were calculated based on the analysis conducted for the daily average values measured at the Coimbra dam-bridge in the period 1990-2004 (Fig. 7).
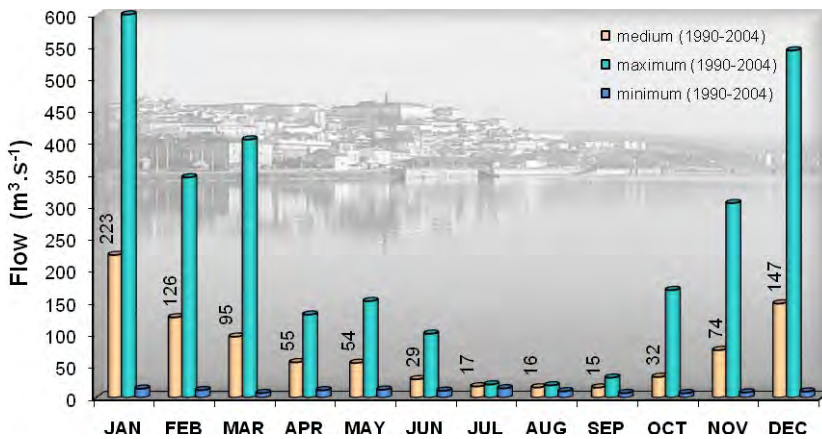


Fig. 7. Average monthly flow observed at  the Coimbra dam-bridge (1990-2004).

Based on this available data, the typical dry-weather flow (corresponding to the 90% percentile on the cumulative flow rate curve) is about 15 $m^3.s^{-1}$, while the annual average flow value was 75 $m^3.s^{-1}$. The maximum flow value for sizing the minor bed of the main channel was estimated about 340  $m^3.s^{-1}$.

The values that were estimated for the Pranto River inflow to the Mondego estuary south arm correspond to those observed during field work, considering the flow discharge curves of the three Alvo sluices (Fig. 8).

So, average daily values of 0 (closed sluices), 15 and 30 $m^3.s^{-1}$ were considered. They correspond, respectively, to discharges carried out during part of the tidal cycle and continuous discharges that are usual in periods of greater rainfall, considering the water demand for existing intensive oriziculture activity in the Pranto river catchment.
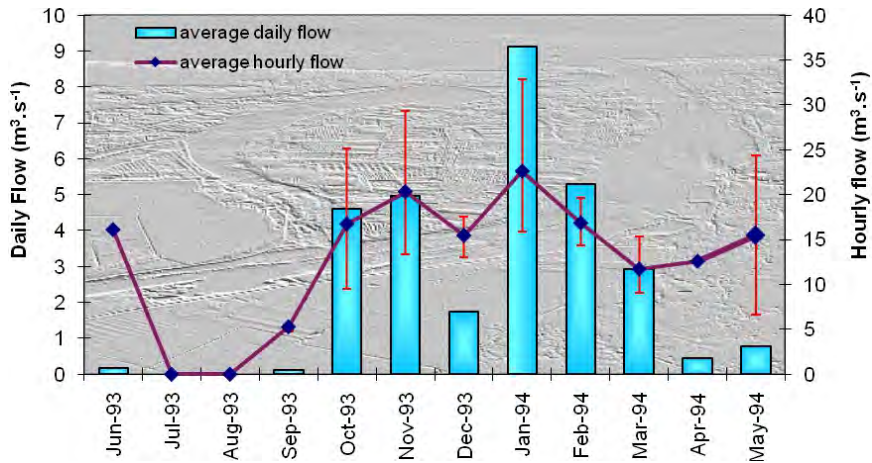
Fig. 8. Pranto river annual (1993-94) flow discharge into the Mondego estuary south arm

In this study, the tidal harmonic signal at Figueira da Foz harbour was generated, for each simulated period, using the programme SR95 (JPL, 1996). Fig. 9 presents an example of a monthly tidal signal used in the *Mondest* model as a downstream boundary condition, during its calibration procedure (Duarte, 2005).
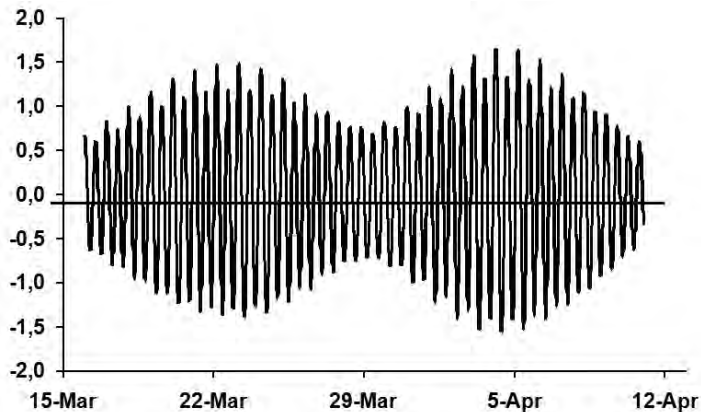


Fig. 9. Monthly tidal harmonic signal at Figueira da Foz harbour using the SR95 programme

## 2.2 Sampling programme

An extensive sampling programme was carried out during last two decades at three benthic stations. The choice of benthic stations was related with the observation of an eutrophication gradient in the south arm of the estuary, involving the replacement of eelgrass, *Zostera noltii* by opportunistic green macroalgae such *as Enteromorpha spp*. and *Ulva spp.*

Water column monitoring was performed by specific sampling campaigns, some of them in simultaneous with the benthic ones, at three other sites: Pranto river mouth (S3); *Armazéns* channel mouth (S2); and Lota (S1), downstream the *Gala* bridge). The location of water

monitoring stations at Mondego estuary south arm were selected in order to represent the different flow regimes observed in this system. Water level, velocity, salinity, temperature and dissolved oxygen were measured in situ and water samples were collected for physical and chemical system characterization.

Dissolved fraction seems to be the most representative of nutrients transport inside the south arm of this estuary, followed by the suspended particulate matter fraction. This finding was very relevant to understand the high eutrophication vulnerability of this sub-system, since these fractions represent the nutrients immediately accessible to the macroalgae tissues incorporation on the growing process.

An example of the sampling programme results is depicted in Figure 10 showing the average monthly values of salinity obtained (in 2000-2001) at Lota station (S1) and Pranto river mouth station (S3), as well as its variation over a medium tidal cycle.
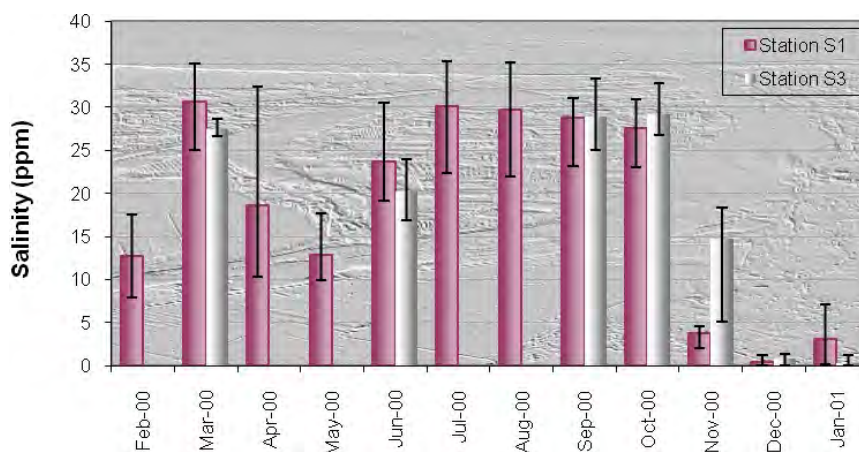


Fig. 10. Average salinity variation in the Mondego estuary south arm (2000-01)

The sampling data analysis was crucial to better understand eutrophication mechanisms and allowed us to conclude that the occurrence of green macroalgae blooms is strongly dependent on the estuarine flushing conditions, salinity gradients and nutrient loading characteristics, availability and residence time (Martins et al., 2001; Duarte et al., 2002).

### 2.3 Dye tracer experiments
Hydrodynamics and pollutant discharge dispersion characteristics are determinant factors in river basin planning and management, where different waters uses and aquatic ecosystems protection must be considered.

Net advection and longitudinal dispersion play important roles in determining transport and mixing of substances and pollutants discharged into the aquatic systems. In order to enhance water sources protection, the knowledge of transport processes is of increasing importance concerning the prediction of the pollutant concentration distribution, particularly when resulting from a continuous or accidental spill event caused by industrial and mining activities or road-river accidents.

Generally, there are two approaches to calculate the transport of solutes in water bodies. One is the more classical calculation based on exact river morphological and hydraulic input

data and the other is the calculation based on estimation of transport parameters such as travel time and dispersion coefficients. Since exact morphological data are often unavailable, the parameter estimation technique is more promising.

In both approaches, tracer experiments are needed to provide field data for water quality models calibration and validation procedures. Indeed, model calibration is often a weak step in its development and using experimental tracer techniques, the calibration and validation problems can be solved satisfactorily, improving the needed feasibility of the early warning systems used by many water supply utilities.

Tracer experiments are typically conducted with artificial fluorescent dyes (like rhodamine WT) (Fig. 11), whose concentrations are easily measured with a fluorometre. These tracers should be easily detected, non toxic and non-reactive, as well as, have high diffusivity, low acidity and sorption for a quasi-conservative behaviour.



Fig. 11. Rhodamine spreading after their injection in a river Mondego reach

Based on field experiments data, many investigators have derived semi-empirical equations (Hubbard et al., 1982; Chapra, 1997; Addler et al., 1999) or applied one-dimensional models (Duarte & Boaventura, 2008) to calculate experimental longitudinal dispersion coefficients from concentration time curves at consecutive sampling sites, using the analytical solution of first order decay kinetics (Table 1).

The injected tracer dye mass must be calculated considering the water volume estimated in the river reach or reservoir system and the fluorometre detection limit. Specific problems of the application of tracers to surface water researches include the photosensitivity of dyes, such as fluorescence tracers, and recovery efficiency, which may imply the use of correction techniques for tracer losses. The tracer mass recovered at each site allowed the assessment of the importance of physical and biochemical river processes by quantifying precipitation, sorption, retention and assimilation losses. Usually, total tracer mass losses resulting from all these sinks can reach 40 to 50% of the injected mass (Duarte & Boaventura, 2008; Addler et al., 1999).

In some recent experiments, a gas tracer ($SF_6$) has been shown to be a powerful tool for examining mixing, dispersion, and residence time on large scales in rivers and estuaries

(Caplow et al. 2004) as an alternative method to dye tracer experiments used for advection and dispersion characterisation.

| MONITORING PROGRAM | REACH | AVERAGE VELOCITY ($ms^{-1}$) | | TRAVEL TIME (h) | | DISPERSION COEFFICIENT ($m^2s^{-1}$) | | RECOVERED MASS (%) |
|---|---|---|---|---|---|---|---|---|
| | | EXPER. | DUFLOW | EXPER. | DUFLOW | EXPER. | DUFLOW | |
| **3 rd.** | S1 – S2 | 0.526 | Var. | 2:37 | 2:35 | 14 | 10 | 57 |
| (Nov.-90) | S2 – S3 | 0.497 | Var. | 2:41 | 2:41 | 51 | 45 | 56 |
| | S3 – S5 | 0.473 | Var. | 3:21 | 3:19 | 37 | 35 | 55 |
| | S1 – S3 | 0.511 | Var. | 5:18 | 5:16 | 34 | - | - |
| | S1 – S5 | 0.497 | Var. | 8:38 | 8:35 | 35 | - | - |
| **1 st.** | S1 – S2 | 1.105 | Var. | 1:14 | 1:14 | 52 | 40 | 62 |
| (Dec.-89) | S2 – S3 | 0.949 | Var. | 1:24 | 1:24 | 61 | 70 | 62 |
| | S1 – S3 | 1.023 | Var. | 2:38 | 2:38 | 58 | - | - |

Table 1. Hydraulic and dispersion parameters estimation using tracer dye experiments in a non-tidal reach of river Mondego

The dispersion processes in rivers are combined with a specific dynamic characterized by a decrease in maximum dye concentration (Fig. 12). The distribution of the tracer in all directions follows the sluggish injection into the channel. In non-tidal rivers, the lateral and vertical dispersion processes are almost always faster than the continuing longitudinal dispersion process.
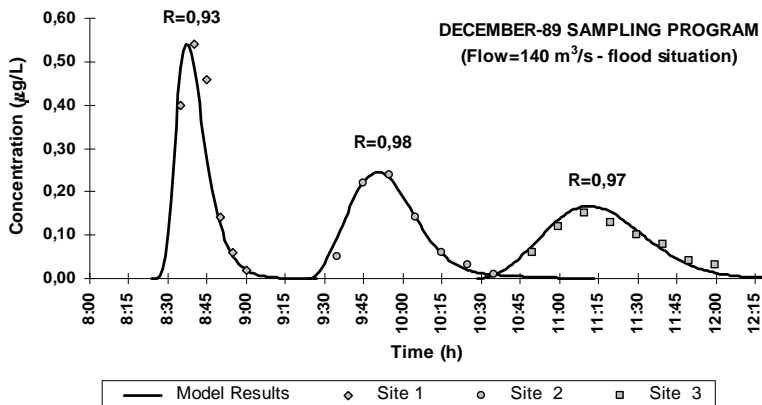


Fig. 12. River Mondego model calibration: correlation between field tracer experiment data and model results.

One-dimensional modelling is a reasonably reliable tool to be considered for estimating the distribution of solutes in large rivers. Complex processes, for example in dead zones or downstream from the confluence of two rivers, have to be investigated by direct measurements and should be described by two-dimensional transport models. Calculation of net advection in tidal rivers is fairly straightforward, but longitudinal dispersion is difficult to determine *a priori*, and the application of two or three-dimensional transport models are often required.

Ever increasing computational capacities provide the development of powerful and user-friendly mathematical models for the simulation and forecast of quality changes in receiving waters after land runoff, mining and wastewater discharges.

The results of several research works have showed that the linkage of tracer experimental approach with mathematical modelling can constitute a power and useful operational tool to establish better warning systems and to improve management practices for the efficiently protection of water supply sources and, consequently, public health.

## 2.4 Mathematical modelling

Numerical modelling is a multifaceted tool that enables a better understanding of physical, chemical and biological processes in the water bodies, based on a "simplified version of the real" described by a set of equations, which are usually solved by numerical methods.

The models to be used for the implementation of the WFD management strategies should ideally have the highest possible degree of integration to comply with the integrated river basin approach, coupling hydrological, hydrodynamic, water quality and ecological modules as a function of the specific environmental issues to analyse.

The *Mondego Estuary (MONDEST)* model was conceptualized (Fig. 13) as an integrated hydroinformatic tool, linking hydrodynamics, water quality and residence time (*TempResid*) modules (Duarte, 2005).
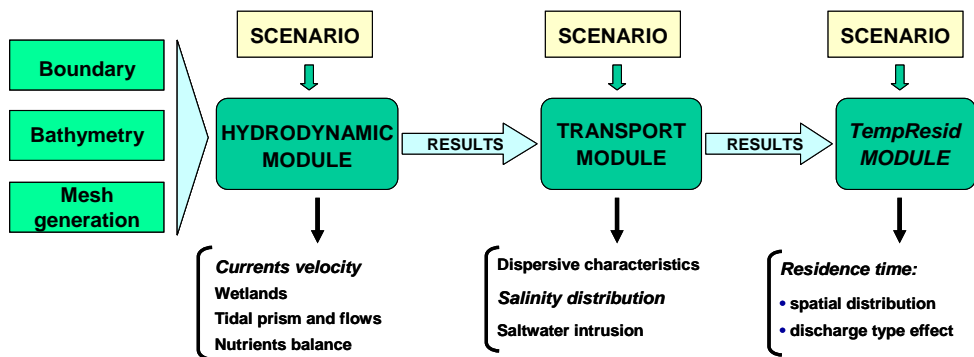


Fig. 13. The *MONDEST* model conceptualization

The formulation of an accurate model requires the best possible definition of the geometry and bathymetry of the water body and the interactions with the boundary conditions, as stated in previous items.

This model is based on generalized computer programmes RMA2 and RMA4 (WES-HL, 1996; 2000), which were applied and adapted to this specific estuarine ecosystem. The CEWES version of RMA4 is a revised version of RMA4 as developed by King & Rachiele (1989).

The RMA2 programme solves depth-integrated equations of fluid mass and momentum conservation in two horizontal directions by the finite element method (FEM) using the Galerkin Method of weighted residuals. The shape (or basis) functions are quadratic for velocity and linear for depth. Integration in space is performed by Gaussian integration. Derivatives in time are replaced by a nonlinear finite difference approximation.

The RMA4 programme solves depth-integrated equations of the transport and mixing process using the Galerkin Method of weighted residuals. The form of the depth averaged transport equation is given by equation (1)

$$h\left(\frac{\partial c}{\partial t} + u\frac{\partial c}{\partial x} + v\frac{\partial c}{\partial y} - \frac{\partial}{\partial x}D_x\frac{\partial c}{\partial x} - \frac{\partial}{\partial y}D_y\frac{\partial c}{\partial y} - \sigma + kc + \frac{R(c)}{h}\right) = 0 \tag{1}$$

Where

h = water depth;

c = concentration of pollutant for a given constituent;

t = time;

u, v = velocity in x direction and y direction;

Dx, Dy, = turbulent mixing (dispersion) coefficient;

k = first order decay of pollutant;

σ = source/sink of constituent;

R(c) = rainfall/evaporation rate.

As with the hydrodynamic model RMA2, the transport model RMA4 handles one-dimensional segments or two-dimensional quadrilaterals, triangles or curved element edges. Spatial integration of the equations is performed by Gaussian techniques and the temporal variations are handled by nonlinear finite differences consistent with the method described for RMA2.

The numerical computation was carried out for all Mondego estuary spatial domains. Several sections were carefully selected and used for calibrating and analysis of the simulation results (Duarte, 2005). The legend includes the designation, section code and their distance to the mouth of the estuary (Fig. 14).
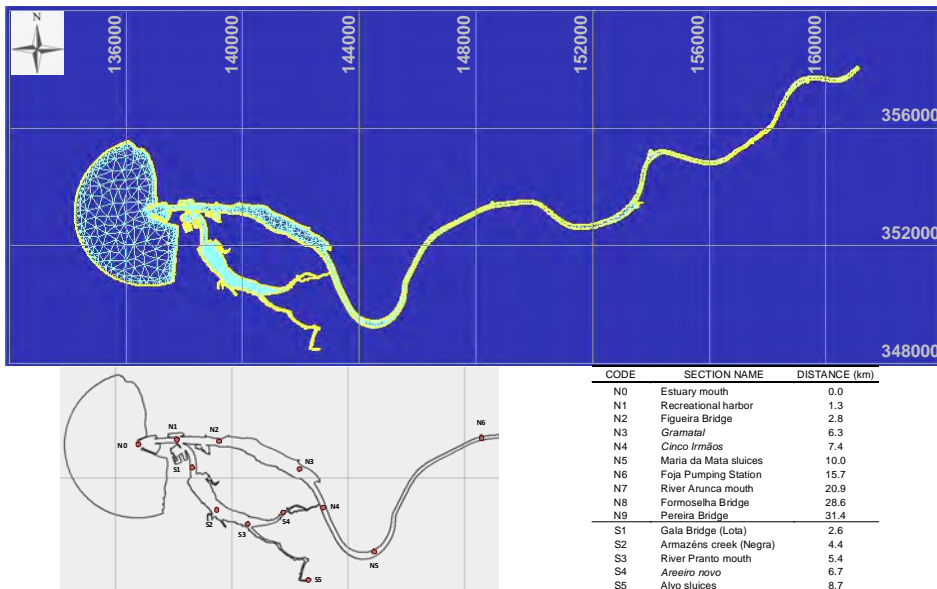


| CODE | SECTION NAME | DISTANCE (km) |
|---|---|---|
| N0 | Estuary mouth | 0.0 |
| N1 | Recreational harbor | 1.3 |
| N2 | Figueira Bridge | 2.8 |
| N3 | *Gramatal* | 6.3 |
| N4 | *Cinco Irmãos* | 7.4 |
| N5 | Maria da Mata sluices | 10.0 |
| N6 | Foja Pumping Station | 15.7 |
| N7 | River Arunca mouth | 20.9 |
| N8 | Formoselha Bridge | 28.6 |
| N9 | Pereira Bridge | 31.4 |
| S1 | Gala Bridge (Lota) | 2.6 |
| S2 | Armazéns creek (Negra) | 4.4 |
| S3 | River Pranto mouth | 5.4 |
| S4 | *Areeiro novo* | 6.7 |
| S5 | Alvo sluices | 8.7 |

Fig. 14. The *MONDEST* model finite elements mesh and outline of the control sections

The size of the elements to consider in the spatial discrimination of the simulated domain of numerical models must be established as a function of larger or smaller spatial gradients than those displayed by the variables (water level and velocity) in that domain. In the case of the Mondego estuary, since the south arm was the preferred object for studying, the network of finite elements was refined in that sub-domain, thereby reducing the maximum area of its (triangular) elements to 500 m² (Duarte, 2005).

In the *MONDEST model*, the hydrodynamic module provides flow velocities and water levels for the water quality module, whose results acts as input on the *TempResid* module, feeding the constituents concentration over the aquatic system. The post-processing and mapping of model results was performed using SMS package (Boss SMS, 1996).

The *TempResid* module was integrally developed in this research work aiming to compute RT values of each water constituent (conservative or not) and allowing to map its spatial distribution over all the estuarine system, considering different simulated management scenarios.

RT value of a substance was calculated for each location and instant, as an interval of time that is necessary for that corresponding initial mass to reduce to a pre-defined percentage of that value. In this work, a value of 10% was adopted for the residual concentration of the substance, attending to the fact that the effect of the re-entry of the mass in the estuary during tidal flooding is considered (a significant effect for dry-weather river flow rates).

The determination of the RT in several stations along the estuary, where the eutrophication gradient occurred, was carried out by applying the *TempResid* programme to the results of the simulations that were performed with the transport module of the MONDEST model. Figure 15 shows an example of the MONDEST model transport module results for the management scenario considered as the most favourable to macroalgae blooms occurrence (Duarte, 2005), due to low freshwater inputs and consequent reduction of estuarine waters renovation (scenario RT1).
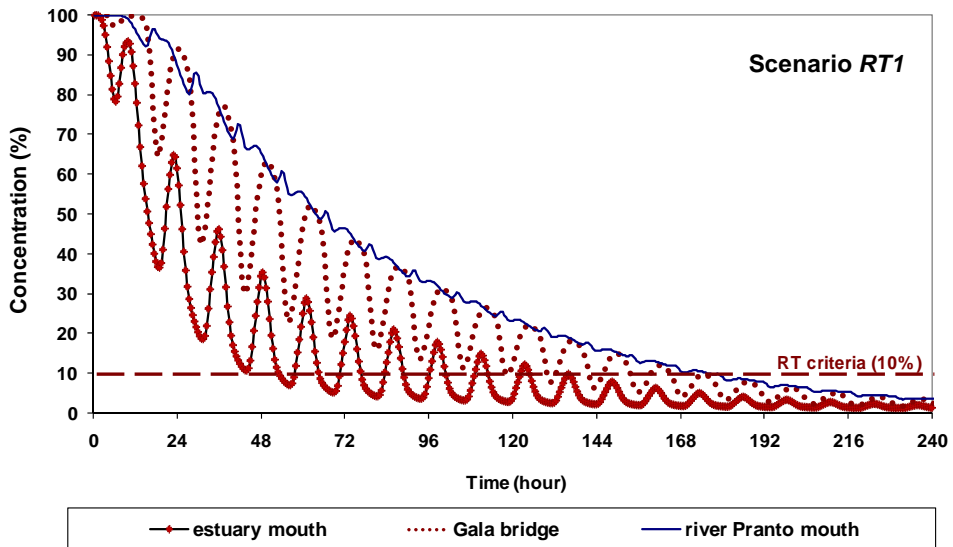


Fig. 15. Residence time computation using *TempResid* module

This graph presents the concentration decrease of a conservative constituent, in three control points (N0 - estuary mouth; S1 - Gala bridge/Lota; and S3- Pranto river mouth), due to estuarine flushing currents, considering the well known re-entrance phenomena at the estuary mouth.

## 2.5 Simulated management scenarios

For hydrodynamic modelling purpose, a wide range (sixteen) of management scenarios were judiciously selected covering a representative set of hydraulic conditions (Table 2), resulting from the combination of typical tidal amplitudes (0.60, 1.15, and 1.60 m) and freshwater flow inputs (from Mondego and Pranto).

| Freshwater flow ($m^3.s^{-1}$) | | TIDE | | |
|---|---|---|---|---|
| Mondego | Pranto | Medium | Spring | Neap |
| | 0 | H 1 | H 2 | H3 |
| 15 | 15 | H 4 | - | - |
| | 30 | H 5 | - | - |
| 75 | 0 | H 6 | H 7 | H 8 |
| | 0 | H 9 | H 10 | H 11 |
| 340 | 15 | H 12 | - | - |
| | 30 | H 13 | - | - |
| 500 | 30 | - | H 14 | - |
| 800 | 30 | - | H 15 | H 16 |

Table 2. Simulated management scenarios for the hydrodynamic modelling

For the *Mondest* transport model calibration and validation, the salinity was adopted as a natural tracer. Several management scenarios (nine) were also carefully selected (Table 3) considering the most representative hydrodynamic conditions in order to estimate salt wedge propagation into the estuary and to identify the areas (in both arms) where favourable salinity values for macroalgae growth can potentiate the estuarine eutrophication vulnerability.

| Freshwater flow ($m^3.s^{-1}$) | | TIDE | | |
|---|---|---|---|---|
| Mondego | Pranto | Medium | Spring | Neap |
| | 0 | SL 1 | SL 6 | SL 9 |
| 15 | 15 | SL 2 | - | - |
| | 30 | SL 3 | - | - |
| 75 | 0 | SL 4 | SL 7 | - |
| 340 | 15 | SL 5 | SL 8 | - |

Table 3. Simulated management scenarios for the hydrodynamic modelling

For the RT values calculation using the *TempResid* module, the simulated management scenarios (fourteen) were defined considering not only the most critical hydrodynamic conditions, but also by carefully selecting distinct pollutant load characteristics (e,g. location, duration and type of the discharge event, instant of tidal cycle when the release occurs) and

constituent decay rates (Table 4) in order to assess and confirm the highest eutrophication vulnerability of the inner areas of the Mondego estuary south arm, due to the expected occurrence of higher RT values.

| SCENARIO | RIVER FLOW ($m^3.s^{-1}$) | | TIDE | LOAD | DECAY RATE ($day^{-1}$) |
|---|---|---|---|---|---|
| | Mondego | Pranto | | | |
| RT 1 | 15 | 0 | medium | point | 0 |
| RT 2 | | | spring | | |
| RT 3 | | | neap | | |
| RT 4 | | | medium | | 1 |
| RT 5 | | | | | 10 |
| RT 6 | | 15 | | | 0 |
| RT 7 | 1 | | | | |
| RT 8 | 75 | | | | |
| RT 9 | 340 | | | | |
| RT 10 | 15 | 0 | | diffuse | 0 |
| RT 11 | | | | | 1 |
| RT12 | 75 | | | | 0 |
| RT 13 | | | | | 1 |
| RT 14 | | | | | 0,5 |

Table 4. Simulated management scenarios for estuarine residence time calculation

In this work only a few examples of the very large amount of MONDEST model results obtained for those different simulated scenarios can be presented. The main aim of the following item will be to highlight the evident influence of hydrodynamics (tidal regime and freshwater inflows) on estuarine residence time spatial variation, which can play a special role in estuarine eutrophication vulnerability assessment.

## 3. Results and discussion

### 3.1 Hydrodynamic modelling

Hydrodynamic modelling results allowed to evaluate the water level and magnitude of currents velocity in both arms during tidal ebbing and flooding situations, and to assess the influence of tidal and freshwater inflows regimes on its variability.

For dry weather conditions, the higher velocity values were obtained in the southern arm, near Gala Bridge, reaching 0.35 (neap tide, scenario H3) to 0.70 m.s$^{-1}$ (spring tide, scenario H2) while in the northern arm these maximum values (which occur in the section N4) are lower, reaching 0.33 (neap tide) to 0.60 m.s$^{-1}$ (spring tide), at 1km upstream the Figueira da Foz bridge. These results are depicted on Figure 16 mapping the effect of extreme tidal regimes on maximum currents velocity magnitude during the flooding period and considering dry-weather conditions.

In the southern arm, the flooding time, which decreases at the inner zones, is much shorter than the ebbing time, due to shallow waters and to large intertidal mudflats areas. This

asymmetry is influenced by the tidal regime and has a fast increase into the inner areas of this arm reaching 2.5 hours: 5 hours for flooding and 7.5 hours for ebbing time. In the northern arm, between the sections N1 and N4, there is a little delay of fifteen minutes in the high tide occurrence and a bigger delay in ebb tide (about two hours).



Fig. 16. Effect of tidal regime on ebbing maximum values of currents velocity magnitude (scenarios H2 and H3)

Figure 17(a) shows an example of the tidal regime effect in the mean velocity magnitude (MVM) variation, at section N4 (where maximum values of this parameter occurred). It should be noted that for a neap tide, the VMM during the tidal flooding period is almost an half of the value reached for a typical sprig tide.

For upstream estuarine sections, water surface levels in high tide are similar, but, in ebb tide, water surface level increases in the inner section due to the effect of the estuarine bathimetry (elevation of bottom level) (Fig. 17b).
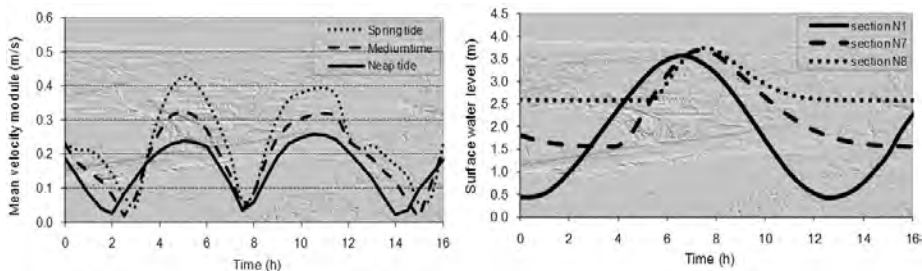


Fig. 17. (a) Effect of tidal regime on ebbing maximum values of currents velocity magnitude (section N4); (b) Surface water level variation along the estuarine system (N1, N7, N8)

### 3.2 Model calibration and validation

The velocities and water levels field data obtained from the sampling programme were used for model calibration and validation. Figure 18 shows an example of a specific procedure performed in section S1 (Gala bridge/Lota) for the parameter "surface water level (SWL)".
Two different sensitivity analyses were carried out to define the accurate values to adopt for the main calibration parameters used in both (hydrodynamic and water transport) modules of *Mondest* model: one for the Manning bottom friction coefficient (n) and horizontal Eddy

viscosity coefficient ($E_h$); and the other for the horizontal dispersion coefficient ($D_h$). For each calibration parameter, three different values were tested comparing field data with the corresponding model results.
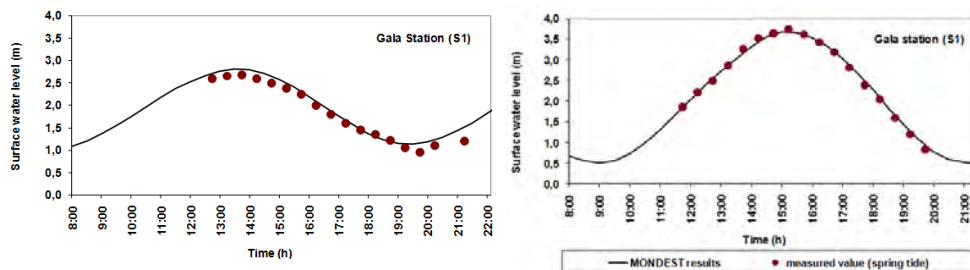


Fig. 18. Hydrodynamic module calibration (spring tide) and validation (neap tide) (station S1)

For the simulated management scenarios and based on calculated correlation coefficients, the best agreements were obtained considering the following parameters values: the ordered pair (n=0.02 $m^{-1/3}$.s; $E_h$= 20 $m^2.s^{-1}$), for the hydrodynamic module; and $D_h$= 30 $m^2.s^{-1}$, for the water transport module.
A more detailed description of these sensitivity analyses (scenarios, results and discussion) can be found in Duarte (2005).

### 3.3 Tidal prism and flow estimation
In this work a new approach was developed for tidal flow estimation, based on the previous tidal prism calculation using mathematical modelling. The adopted approach allows to consider the temporal variation of the cross section area during the tidal cycle and, mainly, the real asymmetry of tidal flooding and ebbing periods verified in the inner estuarine areas. Tidal prisms were calculated as the difference between the water volume in a specific high tide and the correspondent previous ebb tide, which can be automatically given by the query tools of the post-processor module (SMS). Figure 19 shows the spatial variation of tidal
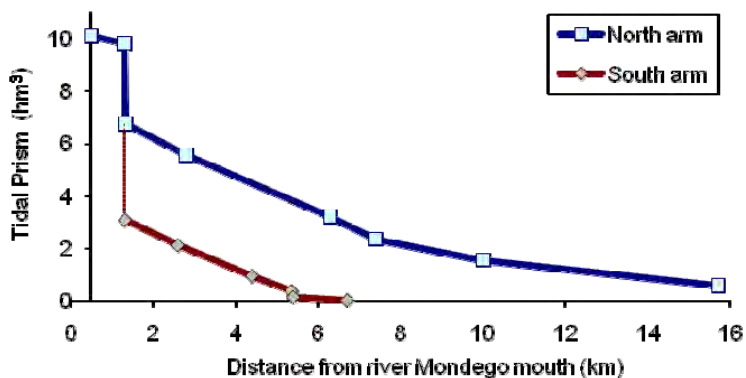


Fig. 19. Tidal prism spatial variation in both estuary arms (flooding of scenario H1)

prism for the both estuary arms (north and south) based on this procedure calculation for each control sections along the Mondego estuary, considering the flooding period of the scenario H1.

The mean tidal flow estimation in each estuarine section can be performed using the correspondents' tidal prism values and the real duration of the ebbing and flood events. The mean tidal flow values obtained for several hydrodynamic scenarios in the sections N0 and S1 are summarized in Table 5.

| Section | Scenario | Tidal prism (hm$^3$) | | Duration (h) | | Mean tidal flow  (m$^3$.s$^{-1}$) | |
|---------|----------|----------|--------|----------|--------|----------|--------|
|         |          | flooding | ebbing | flooding | ebbing | flooding | ebbing |
| **N0** | H 1 | 9.178 | 9.894 | 6.25 | 6.25 | 408 | 440 |
|        | H 2 | 12.02 | 13.063 | 6.25 | 6.25 | 534 | 581 |
|        | H 3 | 5.818 | 5.692 | 6.25 | 6.25 | 259 | 253 |
|        | H 7 | 14.792 | 15.386 | 6,25 | 6,25 | 657 | 684 |
|        | H 10 | 11.387 | 12.089 | 6.00 | 6.50 | 527 | 517 |
| **S1** | H 1 | 2.334 | 2.341 | 5.50 | 7.00 | 118 | 93 |
|        | H 2 | 3.265 | 3.276 | 5.50 | 7.00 | 165 | 130 |
|        | H 3 | 1.269 | 1.266 | 6.00 | 6.50 | 59 | 54 |
|        | H 7 | 3.449 | 345 | 5.50 | 7.00 | 174 | 137 |
|        | H 10 | 3.325 | 3.337 | 5.50 | 7.00 | 168 | 132 |

Table 5. Synthesis of mean tidal flow calculation (sections N0 and S1)

### 3.4 Hydrodynamic influence on estuarine salinity distribution

The analysis of the salinity distribution in the estuary had, as a primary goal, the identification of the areas that, throughout the tidal cycle, present salinity values within the range of 17 to 22‰, defined by Martins et al. (2001) as  the most favourable for algal growth in this specific aquatic ecosystem.

The Pranto river inflow in estuary southern arm has shown a strong influence on salinity distribution decreasing drastically its values to a range far from the one defined as the most favourable for this estuarine eutrophication process. Figure 20 shows the opening Alvo sluices effect on southern arm salinity gradients caused by Pranto river flow discharge of 30 m$^3$.s$^{-1}$, during the ending of ebbing and the beginning of tidal flooding periods (scenarios SL 3 and SL1) (Duarte & Vieira, 2009a).
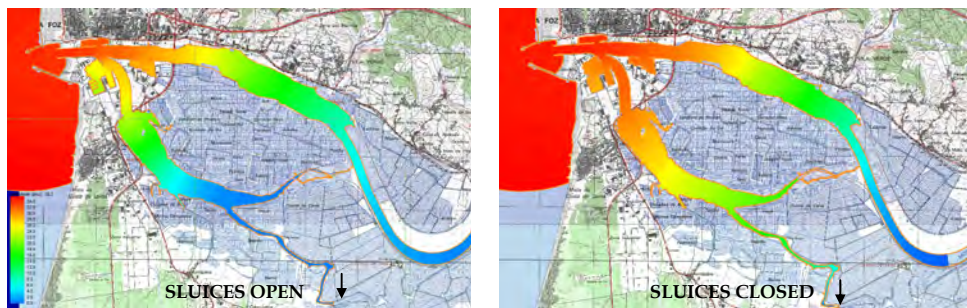


Fig. 20. Effect of Pranto river flow discharge on estuarine salinity distribution (high tide)

The effect of tidal regime on saline wedge propagation into the Mondego estuary can be assessed by comparing the saline front position at high or ebb tide achieved for the extreme tidal amplitudes (spring and neap tides). For the simulated conditions (scenarios SL2 and SL3) a difference of about 4 km in the estuarine saline wedge intrusion was observed: 12.5 km for a spring tide and only 8.5 km for a neap tide. Figure 21 depicts the differences on the saline wedge return (ebb tide) for these two extreme tidal regimes.
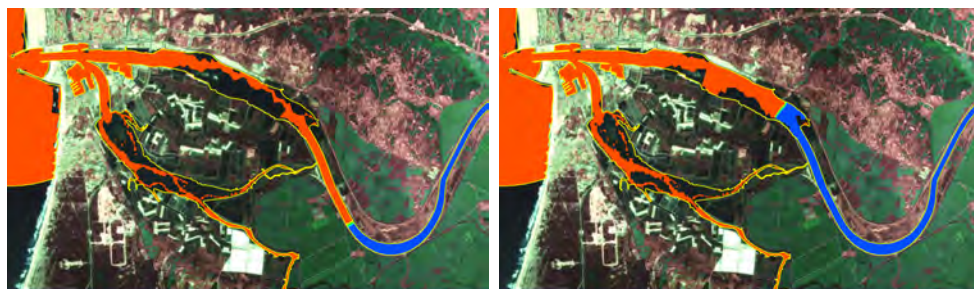


Fig. 21. Effect of tidal regime on saline wedge reflux (ebb tide) (scenarios SL2 and SL3)

### 3.5 Hydrodynamic influence on estuarine residence time distribution

During the warm season (late spring and summer), the Alvo sluices are almost closed (scenario RT1). For this operational condition, the RT values near Pranto mouth station can quintuplicate when compared with those resulting from a Pranto river flow discharge of 15 m³.s⁻¹ (scenario RT6), both under dry-weather conditions (low river Mondego inflows). Figure 22 shows this sensitive increase on flushing capacity of the Mondego estuary south arm due to Pranto river discharges from Alvo sluices opening.



Fig. 22. Effect of Pranto river discharge on RT values distribution (scenarios RT1 and RT6)

For the other hand, when the Alvo sluices remain closed the salinity and the RT values inside the southern arm are strongly influenced by tidal regime. Figure 23 illustrates the gradient of RT spatial distribution, which was mapped applying the *TemResid* module computing availability for the simulation of management scenarios RT2 and RT3.

Simulation results for these two tidal scenarios showed a RT values increase of 50% for a neap tide, when compared with a spring tide, both in the south arm and in the north arm reach, between N1 and N2 control points. This increase is smoothed in the northern arm inner areas, with the lowest increase (only 17%) at the Mondego estuary mouth. The

minimum RT values (3.2 days) occurred in the Mondego estuary mouth (N0) and in the mesotrophic wetland zone of the south arm (near station S2). The maximum RT values (9.5 days) were obtained for the zone (near station S3) with higher eutrophication vulnerability. Concerning the periodicity of tidal regime recurrence, its effect could be very relevant for estuarine biochemical processes with a time scale lower than 6 days.
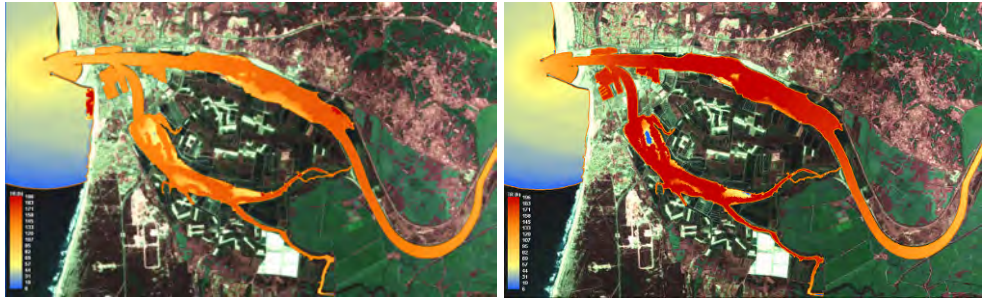


Fig. 23. Effect of tidal regime on RT values distribution (scenarios RT2 and RT3)

## 4. Conclusion

The analysis of the results obtained in the performed simulations allows the confirmation that there is a significant influence of bathymetry in the spatial variation of the RT along the Mondego estuary and consequently, the definition of typical (unique) values for each one of its arms becomes inadequate if they are not associated to local and specific hydrodynamic scenarios.

The results obtained from hydrodynamic modelling have shown a strong asymmetry of ebbing and flooding times in the inner estuary south arm areas due to their complex geo-morphology (extensive wetlands and salt marsh zones, over 75% of its total area). This information allows a better understand of the estuarine circulation pattern, since tide is the major driving force of the southern arm flushing capacity, when the Alvo sluices remain closed. Indeed, the absence of the Pranto river discharge (a typical dry-weather condition) drastically increases salinity and RT values in the inner estuary southern arm and, consequently, the nutrients availability for algae uptake is higher, enhancing estuarine vulnerability to eutrophication.

From the analysis of the results obtained, it is possible to conclude that in both arms of this estuary, the tidal prism volumes are influenced by the bathymetry (extensive wetland areas), tidal regime and freshwater inputs. However, the influence of the tidal regime on the tide prism values is much greater than that of the freshwater inflows, and it is possible to verify that those values do not increase proportionally to the incremental values of the Mondego River flow rate.

The knowledge of the ebbing and flooding duration asymmetry is crucial for a more accurate tidal flow calculation, based on previous tidal prim estimation using mathematical modelling tools. With this new approach for mean tidal flow estimation the variation of cross section area can also be computed increasing the feasibility of the obtained results.

For the simulated conditions a difference of about 4 km in the estuarine saline wedge intrusion was observed: 12.5 km for a spring tide and only 8.5 km for a neap tide. However, a sensitive surface water elevation was monitored in the upper control section (N8), near the

Formoselha bridge (located 30 km upstream the estuary mouth), during a spring tide propagation.

For medium typical tide, drought conditions and conservative constituents, simulation results showed that estuarine RT values range between 6 days (at both arms) and 4 days in the downstream reach of its two arms confluence (control point N1).

The development of integrated methodologies linking tracer experimental approach with hydroinformatic tools (based on 2D and 3D mathematical models) is of paramount interest because they can constitute a accurate and useful operational tool to establish better warning systems and to improve management practices for efficiently protecting water sources and, consequently, public health.

The MONDEST model developed and applied in this work allowed the evaluation and ranking of potential mitigation measures (like nutrient loads reduction or dredging works for hydrodynamic circulation improvement). So, the proposed methodology, integrating hydrodynamics and water quality, constitutes a powerful hydroinformatic tool for enhancing estuarine eutrophication vulnerability assessment, in order to contribute for better water quality management practices and to achieve a true sustainable development.

## 5. References

Addler, M.J.; Stancalie, G. & Raducu, C. (1999). Integrating tracer with remote sensing techniques for determining dispersion coefficients of the Dâmbovita River, Romania. In: *Integrated Methods in Catchment Hydrology – Tracer, Remote Sensing and New Hydrometric Techniques (Proceedings of IUGG 99-Symposium HS4)*, IAHS Publ. No. 258, pp. 75-81, Birmingham, July, 1999.

Bendoricchio, G.D.B. (2006). A water-quality model for the lagoon of Venice, Italy. *Ecological Modelling,* 184, pp. 69–81, ISSN 0304-3800

Boss SMS (1996). *Boss Surface Modeling System-User's Manual*, Brigham Young University Press, USA.

Burwell, D.C. (2001). *Modelling the spatial structure of estuarine residence time : eulerian and lagrangian approaches*. PhD. Thesis, College of Marine Science, University of South Florida, USA.

Caplow, T.; Schlosser, P.; Ho, D. T. & Enriquez, R. C. (2004). Effect of tides on solute flushing from a strait: imaging flow and transport in the East River with $SF_6$. *Environ. Sci. Technol.*, Vol.38, No.17, pp. 4562–4571, ISSN 1520-5851

Chapra, S. C. (1997). *Surface Water Quality Modelling*, McGraw-Hill, New York, USA.

Cucco, A., Umgiesser, G.; Ferrarinb, C.; Perilli A., Canuc, D.M. & Solidoroc, C. (2009). Eulerian and lagrangian transport time scales of a tidal active coastal basin, *Ecological Modelling*, Vol.220, No.7, pp. 913–922, ISSN 0304-3800

Cucco, A. & Umgiesser, G. (2006). Modelling the Venice lagoon water residence time. *Ecological Modelling,* Vol.193, pp. 34–51, ISSN 0304-3800

Cunha, P.P. & Dinis, J. (2002). Sedimentary dynamics of the Mondego estuary. In: *Aquatic ecology of the Mondego river basin. Global importance of local experience,* Pardal M.A., Marques J.C. & Graça M.S. (eds.), pp. 43-62, Coimbra University Press, IBSN 972-8704-04-6, Coimbra, Portugal.

Dronkers, J. & Zimmerman, J.T.F. (1982). Some principles of mixing in tidal lagoons. In: *Oceanologica Acta. Procedings of the International Symposium on Coastal Lagoons*, pp. 107–117, Bordeaux, France, September 9–14, 1981

Dettmann E. (2001). Effect of water residence time on annual export and denitrification of nutrient in estuaries: a model analysis. *Estuaries*, Vol.24, No.4, pp. 481–490, ISSN 1559-2723

Duarte, A.A.L.S. & Vieira, J.M.P. (2009a). Mitigation of estuarine eutrophication proceses by controlling freshwater inflows. In*: River Basin Management V*, ISBN 978-1-84564-198-6, and *WIT Transactions on Ecology and the Environment,* pp. 339-350, ISSN: 1743-3541, WIT Press, Ashusrt, Reino Unido.

Duarte, A.A.L.S. & Vieira, J.M.P. (2009b). Estuarine hydrodynamic as a key-parameter to control eutrophication processes. *WSEAS Transactions on Fluid Mechanics,* Vol.4, No.4, (October 2009), pp. 137-147, ISSN 1790-5087

Duarte, A.A.L.S. & Boaventura, R.A.R (2008). Pollutant dispersion modelling for Portuguese river water uses protection linked to tracer dye experimental data. *WSEAS Transactions on Environment and Development,* Vol.4, No.12, (December 2008), pp. 1047-1056, ISSN 1790-5079

Duarte, A.A.L.S. (2005). *Hydrodynamics influence on estuarine eutrophication processes*. PhD. Thesis, Civil Engineering Dept., University of Minho, Braga, Portugal (in Portuguese).

Duarte, A.A.L.S.; Pinho, J.L.S.; Vieira, J.M.P. & Seabra-Santos, F. (2002). Hydrodynamic modelling for Mondego estuary water quality management. In: *Aquatic ecology of the Mondego river basin. Global importance of local experience,* Pardal M.A., Marques J.C. & Graça M.S. (eds.), pp. 29-42, Coimbra University Press, IBSN 972-8704-04-6, Coimbra, Portugal.

Duarte, A.A.L.S.; Pinho, J.L.S.; Pardal, M.A.; Neto, J.M.; Vieira, J.M.P. & Seabra-Santos, F. (2001). Effect of Residence Times on River Mondego Estuary Eutrophication Vulnerability. *Water Science and Technology,* Vol.44, No.2/3, pp. 329-336, ISSN 0273-1223.

Harremoës, P. & Madsen, H. (1999). Fiction and reality in the modelling world – Balance between simplicity and complexity, calibration and identifiably, verification and falsification. *Water Science and Technology*, Vol.39, No.9, pp. 47–54, ISSN 0273-1223.

Hubbard, E.F.; Kilpatrick, F.A.; Martens, C.A. & Wilson, J.F. (1982). *Measurement of Time of Travel and Dispersion in Streams by Dye Tracing*, Geological Survey, U.S. Dept. of the Interior, Washington, EUA

JPL (1996). *A Collection of Global Ocean Tide Model*s. Jet Propulsion Laboratory, Physical Oceanography Distributed Active Archive Center, Pasadena, CA.

King, I.P. & Rachiele, R.R. (1989). *Program Documentation: RMA4 - A two Dimensional Finite Element Water Quality Model, Version 3.0*, ed. Resource Management Associates, January, 1989.

Luketina, D. (1998). Simple tidal prism model revisited. *Estuarine Coastal and Shelf Science,* Vol.46, pp.77–84, ISSN 0272-7714

Marinov, D. & Norro, A.J.M.Z. (2006). Application of COHERENS model for hydrodynamic investigation of Sacca di Goro coastal lagoon (Italian Adriatic Sea shore). *Ecological Modelling*, Vol.193, No.1, pp. 52–68, ISSN 0304-3800

Monsen, N.E.; Cloern, J.E. & Lucas, L.V. (2002). A comment on the use of flushing time, residence time, and age as transport time scales. *Limnology & Oceanography,* Vol.47, No.5, (May 2002), pp. 1545–1553, ISSN 0024-3590

Oliveira, A. P. & Baptista, A.M. (1997). Diagnostic modelling of residence times in estuaries. *Water Resources Reseach*, Vol.33, pp.1935–1946, ISSN 0024-3590

Paerl, H.W (2006). Assessing and managing nutrient-enhanced eutrophication in estuarine and coastal waters: interactive effects of human and climatic perturbations. *Ecological Engineering,* Vol.26, No.1, (January 2006), pp. 40-54, ISSN 0925-8574

Pardal, M.A.; Cardoso, P.G.; Sousa, J.P.; Marques, J.C. & Raffaelli, D.G. (2004). Assessing environmental quality: a novel approach. *Marine Ecology Progress Series,* Vol.267, pp. 1-8, ISSN 0171-8630.

Sanford, L.; Boicourt, W. & Rives, S. (1992). Model for estimating tidal flushing of small embayments. *Journal of Waterway, Port, Coastal and Ocean Engineering,* Vol.118, No.6, pp. 913–935, ISSN 1943-5460

Stamou, A.I.; Nanou-Giannarou, K. & Spanoudaki, K. (2007). Best modelling practices in the application of the Directive 2000/60 in Greece. *Proceedings of the 3rd IASME/WSEAS Int. Conference on Energy, Environment, Ecosystems and Sustainable Development*, pp. 388-397, Agios Nikolaos, Crete Island, Greece, July 24-26, 2007.

Takeoka, H. (1984). Fundamental concepts of exchange and transport time scales in a coastal sea. *Continental Shelf Research,* Vol.3, No.3, pp. 311–326, ISSN 0278-4343

Thomann, R.V. & Linker, L.C. (1998). Contemporary issues in watershed and water quality modelling for eutrophication control. *Water Science & Technology*, Vol.37, pp. 93-102, ISSN 0273-1223

Valiela, I., McClelland, J., Hauxwell, J., Behr, P.J., Hersh, D. & Foreman, K. (1997) Macroalgae blooms in shallow estuaries: controls, ecophysiological and ecosystem consequences. *Limnology & Oceanography,* Vol.42, No.5, (January 1997), pp. 1105–1118, ISSN 0024-3590

Vieira, J.M.P; Duarte, A.A.L.S.; Pinho, J.L.S. & Boaventura, R.A. (1999). A Contribution to Drinking Water Sources Protection Strategies in a Portuguese River Basin, *Proceedings of the XXII World Water Congress,* CD-Rom, Buenos Aires, Argentina, September, 5-7, 1999.

Wang, C.F.; Hsu,M. & Kuo, A.Y.(2004). Residence time of the Danshuei Estuary, Taiwan. *Estuarine, Coastal and Shelf. Science,* Vol.60, pp. 381-393, ISSN 1906-0015

WES-HL (1996). *Users Guide to RMA2 Version 4.3.* US Army Corps of Engineers, Waterways Experiment Station Hydraulics Laboratory, Vicksburg, USA.

WES-HL (2000). *Users Guide to RMA4 WES Version 4.5.* US Army Corps of Engineers, Waterways Experiment Station Hydraulics Laboratory, Vicksburg, USA.